Can we forecast the arrival of ICMEs for the whole Heliosphere?

Dario Del Moro[1], **Gianluca Napoletano**[1], **Francesco Berrilli**[1], **Luca Giovannelli**[1], **Ermanno Pietropaolo**[2], and **Raffaello Foldes**[2]

[1]Physics Department, University of Rome "Tor Vergata", Via Cracovia, 50, 00133 Roma RM, IT
[2]Chemistry and Physics Department, University of L'Aquila, Via Vetoio , 67100 Coppito AQ, IT

Solar wind transients, i.e. interplanetary coronal mass ejections (ICMEs) drive Space Weather throughout the heliosphere and the prediction of their impact on different solar system bodies is one of the primary goals of the Planetary Space Weather forecasting. We realized a procedure based on the Drag-Based Model (1, 2) which uses probability distributions for the input parameters, and allows the evaluation of the uncertainty on the forecast. This approach has been tested against a set of ICMEs whose transit times are known, obtaining extremely promising results. We apply this model to propagate a sample of ICMEs from their sources on the solar surface into the heliosphere. We made use of the seminal works by Prise et al. (3), Winslow et al. (4) and Witasse et al. (5) who tracked the ICMEs through their journeys using data from several spacecraft. Considering the extremely short computation time needed by the model to propagate ICMEs, this approach is a promising candidate to forecast ICME arrival to planetary bodies and spacecraft in the whole heliosphere, with relevant application to space-mission short-term planning.

Heliosphere | Coronal Mass Ejection (CME) | Space Weather
Correspondence: *delmoro@roma2.infn.it*

Fig. 1. The probability distributions used in the PDBM are derived from past data: a Log-Normal PDF for the drag parameter, Gaussian PDFs associated to the measure errors for the CME initial position and velocity, two different Gaussian PDFs for the solar wind, for the case of fast or slow solar wind (decided checking for coronal holes in the proximity of the CME source). From the ICME arrival condition sets, we compute our best estimate and the associated error for ICME time and velocity at arrival.

Introduction.

Coronal Mass Ejections (CMEs) are expulsion of plasma from the Sun with repercussions on the whole interplanetary space and are responsible for major geomagnetic storms. The accurate prediction of the arrival time of Interplanetary Coronal Mass Ejections (ICMEs) at Earth and more recently elsewhere in the heliospgere, has always been a primary goal of the space-weather forecasting (6, 7). Modeling and forecasting methods can be divided into several classes.

- Purely empirical/statistical methods making use of relationships established between coronagraphically measured parameters and measured heliospheric propagation characteristics of past ICMEs.

- Numerical MHD-based models of the heliospheric propagation of the ICME.

- Kinematic models that apply a somewhat simplified description of the main interaction the ICME is subject to during its interplanetary journey.

In this work we employ a model belonging to the last category, the Probabilistic Drag-Based Model (PDBM, henceforth 2). The PDBM makes use of probability distribution functions (PDFs), rather than exact values, as input parameters,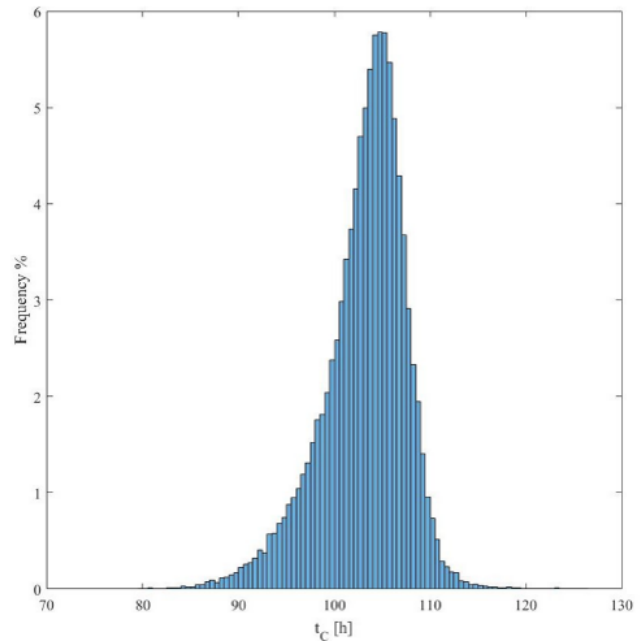 to model the CME propagation in the interplanetary space, allowing us to forecast ICME arrival times and velocities and to evaluate also the uncertainty on the forecast.

The Model.

The PDBM returns a statistical evaluation of the time of arrival and velocity of the ICME at a chosen distance from the Sun, transforming the probability or error distribution functions associated to the input parameters into PDF for the output results. This allows computing the best estimates and the errors for both the time of arrival and the velocity of a given ICME. For each ICME whose initial position (r0) and velocity (v0) are measured with a certain precision, we will generate N different [r0, v0, ω, γ] initial conditions sets (ω is the solar wind speed and γ is the drag parameter in eq. 2 in 2), randomly chosen from the relative PDFs, to compute the transit time and the velocity at a target P. This process generates the PDFs associated to t_P and v_P, which can be used to estimate the ICME most probable time of arrival and velocity and their associated uncertainties at P. Details and extended description in Napoletano et al. (2).
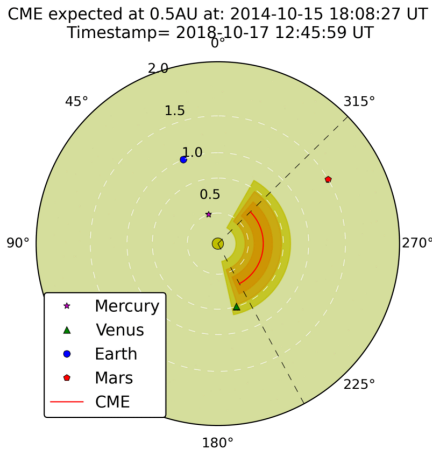
CME expected at 0.5AU at: 2014-10-15 18:08:27 UT
Timestamp= 2018-10-17 12:45:59 UT

Fig. 2. Output of the PDBM: the estimated CME propagation path in the inner heliosphere (until ∼ 3 AU) is represented by dashed lines, and the CME itself is represented by different shades of colors, representing different confidence levels of the CME extension: yellow=10% probability, light orange=50% probability, dark orange=90% probability. Planets are represented by colored symbols. This view shows the ICME hitting both Venus and Mars.

PDBM applied on data from "Interplanetary coronal mass ejection observed at STEREO-A, Mars, comet 67P/Churyumov-Gerasimenko, Saturn, and New Horizons en route to Pluto: Comparison of its Forbush decreases at 1.4, 3.1, and 9.9 AU" by Witasse et al. (5) .

A powerful CME erupted from Solar Active Region 12192 on 14 October 2014 at around 18:30 UT. The journey of this ICME was studied in detail with in situ data sets acquired by eight spacecraft and one rover.
The ICME passed by the STEREO-A spacecraft, Mars, comet 67P/Churyumov-Gerasimenko (C67 henceforth), Saturn, and apparently New Horizons on its way to Pluto. The paper by Witasse et al. (5) described the propagation of this ICME out to 32AU and also investigated whether the ICME was observed also by Voyager 2 in late March 2016 at ∼ 111 AU.
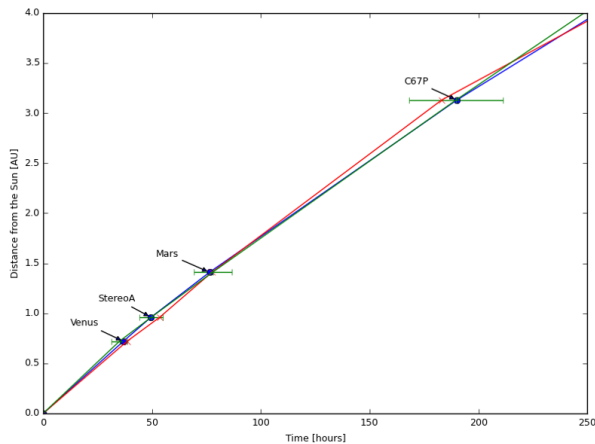
In that work, the propagation of the ICME, was simulated via the WSA-ENLIL Cone model (8, 9) available from the Community Coordinated Modeling Center (10). The CME parameters used for the model input were radial speed 1015 km/s, longitude -150°, latitude -12°, and full width 116° (in agreement with the CGS 11, fitting results of the CME expulsion). The simulations initialized with these parameters produced output with a reasonable match to in situ observation. The ICME propagation was also reproduced via a DBM based online tool developed by the Centre de Données de la Physique des Plasmas (CDPP propagation tool, http://propagationtool.cdpp.eu/), whose results agreed with ENLIL simulations, although with different speeds as inputs (but within the error range of the GCS measurements).

Using the same input parameters as the WSA-ENLIL+Cone simulation, we re-run the ICME propagation with the PDBM. Some of the outputs are shown here. In Figg. 3 and 4, in particular, we compare the PDBM forecast arrival times at different targets (green line) against the WSA-ENLIL forecast arrival times (red line) and the actual arrival times assessed by the different in situ measures (blue line). In this case, the PDBM performs extremely well, since the forecast arrival times are always close to the actual arrival times and in any case well within the forecast 1σ error bars. As can be expected, the PDBM fails instead to predict the arrival time at Voyager 2 spacecraft. The forecast is largely in advance of the actual arrival time. It is worth to remember that Voyager 2 in the 2016 was inside the Heliopause, where the hypothesis of a free streaming solar wind is probably no more valid.

The time needed to compute the N=10000 model runs for this PDBM simulation is less than one minute (including the Voyager 2 position!).
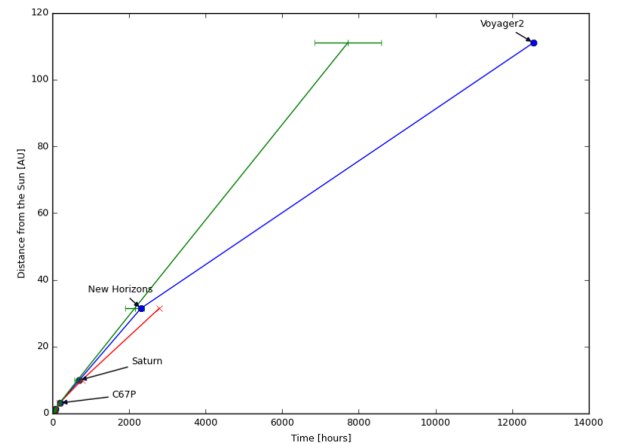

Fig. 3. Comparison between ICME transit times at different targets in the heliosphere from the Sun to ∼ 4AU. In blue the measured times, in red the time forecast by the WSA-Enlil simulation, in green (with error bars) the time forecast by the PDBM.

Fig. 4. Comparison between ICME transit times at different targets in the heliosphere from ∼ 3AU to ∼ 120AU. In blue the measured times, in red the time forecast by the WSA-Enlil simulation, in green (with error bars) the time forecast by the PDBM.

CME expected at 0.31AU at: 2010-06-20 22:53:53 UT
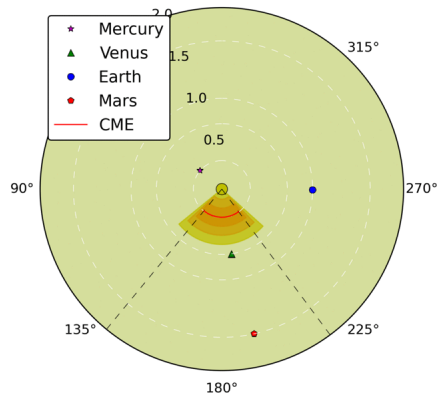Timestamp= 2018-10-26 11:48:01 UT

Fig. 5. Output of the PDBM: the estimated CME propagation path in the inner heliosphere (until 3 AU) is represented by dashed lines, and the CME itself is represented by different shades of colors, representing different confidence levels of the CME extension: yellow=10% probability, light orange=50% probability, dark orange=90% probability. Planets are represented by colored symbols. This view shows the ICME hitting both Venus and Mars.

PDBM applied on data from "Analysis of a coronal mass ejection and corotating interaction region as they travel from the Sun passing Venus, Earth, Mars, and Saturn" by Prise et al. (3)..

A CME erupted from the Sun at 01:30 UT on 20 June 2010, with v≈628 km/s. On board STEREO, its eruption was observed by the SECCHI (12) instrument suite, on-disk by the Extreme Ultraviolet Imager (EUVI 13) and propagating away from the Sun by the Cor-1 and Cor-2 (14) coronagraphs and the Heliospheric Imagers (HI 15). From the Earth side, the CME was imaged on-disk by the Atmospheric Imaging Assembly (AIA 16) on SDO and off the Sun with the Large Angle and Spectrometric Coronagraph (LASCO 17) experiment on SOHO (18). A corotating interaction region (CIR) interacted with the CME during its propagation. CIRs

are formed when a region of fast solar wind catches up with a region of slow solar wind creating a density enhancement at the interface between them, known as a stream interaction region (SIR). The CIR was detected by in situ instruments on Venus express, on STEREO-B and at Mars. Both the ICME and the CIR were simulated using the ENLIL prediction model. The simulation predicted that the ICME merged with the CIR beyond the orbit of Mars, and reaches Saturn as a SIR.

As in the case above, we re-run the ICME propagation with the PDBM, using the same input parameters as the ENLIL simulation. In Figg. 6 and 7, we compare the PDBM forecast arrival times at different targets (green line) against the WSA-ENLIL fore-cast arrival times (red line) and the actual arrival times assessed by the different in situ measures (blue line).

In this ICME propagation, the PDBM is successful in prediction the arrival times at Venus and Stereo B (discrepancies wrt to measures are well within the 1σ error bars), but fails to predict the arrival times at Mars and Saturn. The PDBM forecasts at Mars and Saturn are largely behind the actual arrival dates. We interpret this delay with the CIR interacting with the ICME before the reaching of Mars orbit and therefore effectively generating a SIR that passed by these outer planets.
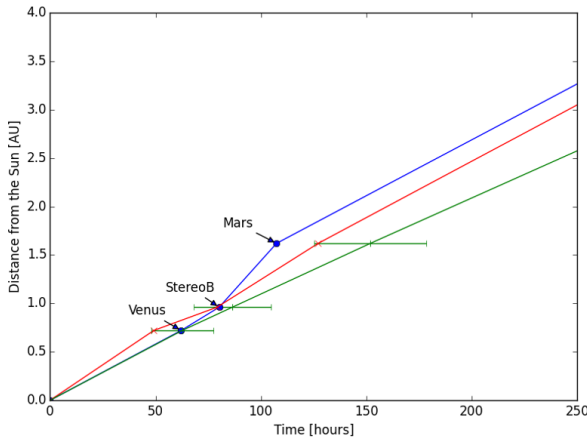

Fig. 6. Comparison between ICME transit times at different targets in the heliosphere from the Sun to ∼ 4AU. In blue the measured times, in red the time forecast by the WSA-Enlil simulation, in green (with error bars) the time forecast by the PDBM

Fig. 7. Comparison between ICME transit times at different targets in the heliosphere from ∼ 3AU to ∼ 14AU. In blue the measured times, in red the time forecast by the WSA-Enlil simulation, in green (with error bars) the time forecast by the PDBM.
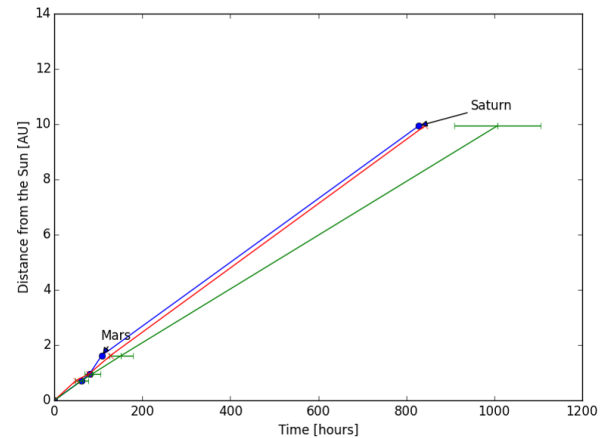
PDBM applied on data from "Interplanetary coronal mass ejections from MESSENGER orbital observations at Mercury" by Winslow et al. (4).

We make use of a catalog of ICME events observed by the MESSENGER Magnetometer (19), in orbit around Mercury from 2011 to 2014, to investigate interplanetary coronal mass ejections (ICMEs) near 0.3 AU. For each of these ICMEs, the most likely CME counterpart at the Sun was identified, by using SOHO/LASCO (17) and STEREO/SECCHI coronagraph (12) observations. This allowed the inclusion in the ICME catalog of the average transit speeds from the Sun to Mercury; the CME launch times and approximate CME launch speeds.

Using these information, we were able to compute PDBM simulations for the 61 ICMEs in the catalog and to perform a statistical study of the results. in Fig. 8, we plot the transit time forecast against the actual transit time for each ICME in the catalog. As always, PDBM forecast are associated with an error estimation, represented by the 1σ error bar in the plot. Also, we plotted as a blue shadowed area the region were the match between forecast and reality is within the statistical errors due to the estimation of the CME launch parameters (time, position and velocity).

Apparently, the PDBM is performing extremely well for the fast ICMEs, but it seems to be slightly biased towards forecasting in advance for the slower CMEs. A possible explanation may be a systematic difference between CMEs faster or slower than the Solar Wind. We are at present investigating this hypothesis with hydrodynamic simulations, and larger ICME datasets (e.g. 20).
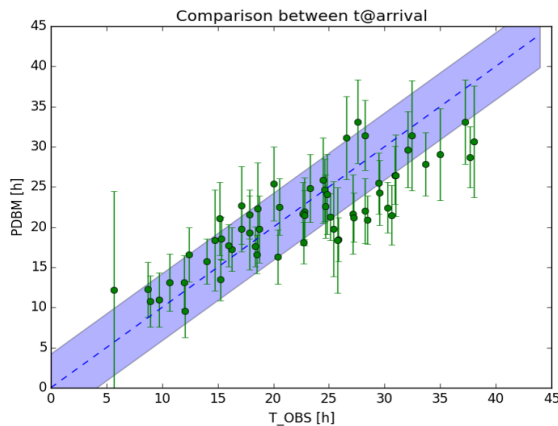

Fig. 8. Dots with error bars are the forecast transit times versus observed transit time of the ICMEs observed by the Messenger mission orbiting Mercury during 2011-2015. The dashed line shows the perfect match expectation, with the 1σ travel time measure error zone shaded in blue.

Conclusions.

Can we forecast the arrival of ICMEs for the whole Heliosphere?
Yes, taking into account some limitations and coping with measure errors.

It takes a relatively long time to obtain a single MHD or even HD simuation of the propagation of an ICME into the Heliosphere up to ~10 or ~100 AU. Also, the uncertainty in the near-Sun boundary conditions, rather than model physics or numerics, often results in large forecast errors. At present, ensembles of ~100 heliospheric model runs with perturbed initial conditions are used to estimate the forecast uncertainty, but it is not feasible to thoroughly explore the high-dimensional parameter space with such models considering distances much larger than 1 AU.

We presented in this display three case applications where the PDBM obtained nice and promising results. The PDBM employs a statistical approach for the computation of kinematic propagation of ICME, making use of PDFs to cope with our lack of knowledge on CME or IMF parameters. It is computationally inexpensive: it can estimate CME arrival at a > 100 AU distant target using a large ensemble in seconds on a laptop. Even for ICME impacting on Mercury, in most of the cases a forecast could be available in time to upload a particular instrumental configuration or to put the spacecraft in safe mode.

Also, the PDBM could serve as an explorer, data-assimilation model, since it could run ensembles of 10^4 to 10^6 simulations to identify those promising regions of the parameter space to be later investigated in more detail by the full MHD models models.

Bibliography

1. Bojan Vršnak, Tomislav Žic, Dijana Vrbanec, Manuela Temmer, Tanja Rollett, Christian Möstl, Astrid Veronig, Jaša Čalogović, Mateja Dumbović, Slaven Lulić, et al. Propagation of interplanetary coronal mass ejections: The drag-based model. *Solar physics*, 285(1-2):295–315, 2013.
2. Gianluca Napoletano, Roberta Forte, Dario Del Moro, Ermanno Pietropaolo, Luca Giovannelli, and Francesco Berrilli. A probabilistic approach to the drag-based model. *Journal of Space Weather and Space Climate*, 8:A11, 2018.
3. AJ Prise, LK Harra, SA Matthews, Chris S Arridge, and Nick Achilleos. Analysis of a coronal mass ejection and corotating interaction region as they travel from the sun passing venus, earth, mars, and saturn. *Journal of Geophysical Research: Space Physics*, 120(3):1566–1588, 2015.
4. Reka M Winslow, Noé Lugaz, Lydia C Philpott, Nathan A Schwadron, Charles J Farrugia, Brian J Anderson, and Charles W Smith. Interplanetary coronal mass ejections from messenger orbital observations at mercury. *Journal of Geophysical Research: Space Physics*, 120(8):6101–6118, 2015.
5. Olivier Witasse, Beatriz Sánchez-Cano, ML Mays, P Kajdič, Hermann Opgenoorth, HA Elliott, IG Richardson, I Zouganelis, J Zender, RF Wimmer-Schweingruber, et al. Interplanetary coronal mass ejection observed at stereo-a, mars, comet 67p/churyumov-gerasimenko, saturn, and new horizons en route to pluto: Comparison of its forbush decreases at 1.4, 3.1, and 9.9 au. *Journal of Geophysical Research: Space Physics*, 122(8):7865–7890, 2017.
6. Ioannis A Daglis. Space storms, ring current and space-atmosphere coupling. In *Space storms and space weather hazards*, pages 1–42. Springer, 2001.
7. Carolus J Schrijver and George L Siscoe. *Heliophysics: space storms and radiation: causes and effects*. Cambridge University Press, 2010.
8. CN Arge, JG Luhmann, D Odstrcil, CJ Schrijver, and Y Li. Stream structure and coronal sources of the solar wind during the may 12th, 1997 cme. *Journal of Atmospheric and Solar-Terrestrial Physics*, 66(15-16):1295–1309, 2004.
9. D Odstrcil. Modeling 3-d solar wind structure. *Advances in Space Research*, 32(4):497–506, 2003.
10. CCMC Team. Community coordinated modeling center, 2020.
11. AFR Thernisien, RA Howard, and A Vourlidas. Modeling of flux rope coronal mass ejections. *The Astrophysical Journal*, 652(1):763, 2006.
12. Russell A Howard, JD Moses, Angelos Vourlidas, JS Newmark, Dennis G Socker, Simon P Plunkett, Clarence M Korendyke, JW Cook, A Hurley, JM Davila, et al. Sun earth connection coronal and heliospheric investigation (secchi). *Space Science Reviews*, 136(1-4):67, 2008.
13. Jean-Pierre Wülser, James R Lemen, Theodore D Tarbell, C Jacob Wolfson, Joseph C Cannon, Brock A Carpenter, Dexter W Duncan, Glenn S Gradwohl, Syndie B Meyer, Augustus S Moore, et al. Euvi: the stereo-secchi extreme ultraviolet imager. In *Telescopes and Instrumentation for Solar Astrophysics*, volume 5171, pages 111–122. International Society for Optics and Photonics, 2004.
14. William T Thompson, Joseph M Davila, Richard R Fisher, Larry E Orwig, John Eric Mentzell, Samuel E Hetherington, Rebecca J Derro, Robert E Federline, David C Clark, Philip TC Chen, et al. The cor1 inner coronagraph for stereo-secchi. In *Innovative Telescopes and Instrumentation for Solar Astrophysics*, volume 4853, pages 1–11. International Society for Optics and Photonics, 2003.
15. CJ Eyles, RA Harrison, Chris J Davis, NR Waltham, BM Shaughnessy, HCA Mapson-Menard, Danielle Bewsher, SR Crothers, JA Davies, GM Simnett, et al. The heliospheric imagers onboard the stereo mission. *Solar Physics*, 254(2):387–445, 2009.
16. James R Lemen, David J Akin, Paul F Boerner, Catherine Chou, Jerry F Drake, Dexter W Duncan, Christopher G Edwards, Frank M Friedlaender, Gary F Heyman, Neal E Hurlburt, et al. The atmospheric imaging assembly (aia) on the solar dynamics observatory (sdo). In *The solar dynamics observatory*, pages 17–40. Springer, 2011.
17. GE Brueckner, RA Howard, MJ Koomen, CM Korendyke, DJ Michels, JD Moses, DG Socker, KP Dere, PL Lamy, A Llebaria, et al. The large angle spectroscopic coronagraph (lasco). In *The SOHO Mission*, pages 357–402. Springer, 1995.
18. V Domingo, B Fleck, and Arthur I Poland. The soho mission: an overview. *Solar Physics*, 162(1-2):1–37, 1995.
19. Brian J Anderson, Mario H Acuña, David A Lohr, John Scheifele, Asseem Raval, Haje Korth, and James A Slavin. The magnetometer instrument on messenger. In *The MESSENGER mission to Mercury*, pages 417–450. Springer, 2007.
20. Ian G Richardson and Hilary V Cane. Near-earth interplanetary coronal mass ejections during solar cycle 23 (1996–2009): Catalog and summary of properties. *Solar Physics*, 264(1):189–237, 2010.
21. Dario Del Moro, Gianluca Napoletano, Roberta Forte, Luca Giovannelli, Ermanno Pietropaolo, and Francesco Berrilli. Forecasting the 2018 february 12th cme propagation with the p-dbm model: A fast warning procedure. *Annals of Geophysics*, 62(4):456, 2019.

Supplementary Note 1: The Drag Based Model

The drag-based model relies on the hypothesis that all the interactions responsible for the launch of the CME cease in the upper corona, and that, beyond a certain distance, the dynamics of ICME propagation are governed mainly by its interaction with the ambient solar wind. The DBM considers such an interaction by means of a drag force analogous to that experienced by a body immersed in a fluid. The idea of an MHD analogous "hydrodynamical" drag is supported by the observation that ICMEs which are faster than the solar wind are decelerated, whereas those slower than the solar wind are accelerated by the ambient flow (1, 2).

Following Cargill (3), we consider the relative speed dependence of the drag force in the radial direction:

$$F_d = -C_d A \rho (v - w)|v - w| \tag{S1}$$

where v is the ICME radial speed and w that of the solar wind, A is the ICME cross-section, ρ is the solar wind density and C_d is an dimensionless coefficient for the drag force. In a classical Newton's law framework, this leads to a radial drag acceleration in the form:

$$a = -\gamma(v - w)|v - w| \tag{S2}$$

where γ is the so-called *drag parameter* which contains the information about the ICME shape, mass, and in general about the effectiveness of the drag effect.

Considering the solar wind speed and the drag parameter as constants (which is a good approximation beyond $20 - 40\, R_\odot$. See 3, 4), equation (S2) can be solved explicitly, obtaining as functions of time the ICME speed:

$$v(t) = \frac{v_0 - w}{1 \pm \gamma(v_0 - w)t} + w \tag{S3}$$

and the heliospheric distance:

$$r(t) = \pm\frac{1}{\gamma} \ln \left[1 \pm \gamma(v_0 - w)t \right] + wt + r_0 \tag{S4}$$

where the $\pm$ signs apply to the cases $v_0 > w$ and $v_0 < w$, respectively, and r_0 and v_0 are the CME distance from the Sun and velocity at the onset time t_0. In this framework, the model needs four quantities, $[r_0, v_0, w, \gamma]$, to compute the heliospheric distance and velocity of the ICME at any t.

The shape of the ICME we are modeling corresponds to type A) in Fig.9 of Schwenn et al. (5), i.e. the front of the CME is a section of a sphere concentric with the Sun.

Supplementary Note 2: the Probabilistic Drag Based Model

As just stated, the DBM needs four quantities to be computed, namely $[r_0, v_0, w, \gamma]$. The first two quantities suffer from measure errors, while the last two are, in general, unknown.

If we consider the measure errors to be described by Gaussian PDFs, and assume a priori PDFs for both w and γ, we can extend the DBM into a probabilistic approach.

The Probabilistic drag-based model (P-DBM henceforth), is a Monte-Carlo evaluation of the time of arrival and the velocity of the ICME at a chosen distance from the Sun, transforming the PDFs associated to the inputs into PDFs for the outputs, thus generating best estimates and errors for both the time of arrival and the velocity. For each ICME whose r_0 and v_0 are measured, we can generate N different $[r_0, v_0, w, \gamma]$ initial conditions sets, randomly chosen from the relative PDFs, to compute via eqs. (S3) and (S4) the transit time and the velocity at 1 AU, for example. This process generates the PDFs associated to t_{1AU} and v_{1AU}, which can be used to estimate the ICME most probable time of arrival and velocity and their associated uncertainties at 1 AU.

Of course, the robustness of the results strongly depends on the validity of the assumptions, the realism of the PDFs, and on a thorough exploration of the parameter space, i.e. how large is N. Given the simplicity of eq. (S3) and (S4) and the present computing capabilities, N of the order of $10^4 - 10^6$ can be used to explore the parameter space and obtain nicely sampled output PDFs in a matter of seconds (see examples in Fig. S4).

A. Probability Distribution Functions. The probability distributions used in the PDBM are derived from past data: a Log-Normal PDF for the drag parameter, Gaussian PDFs associated to the measure errors for the CME initial position and velocity, two different Gaussian PDFs for the solar wind, for the case of fast or slow solar wind (decided checking for coronal holes in the proximity of the CME source). From the ICME arrival condition sets, we compute our best estimate and the associated
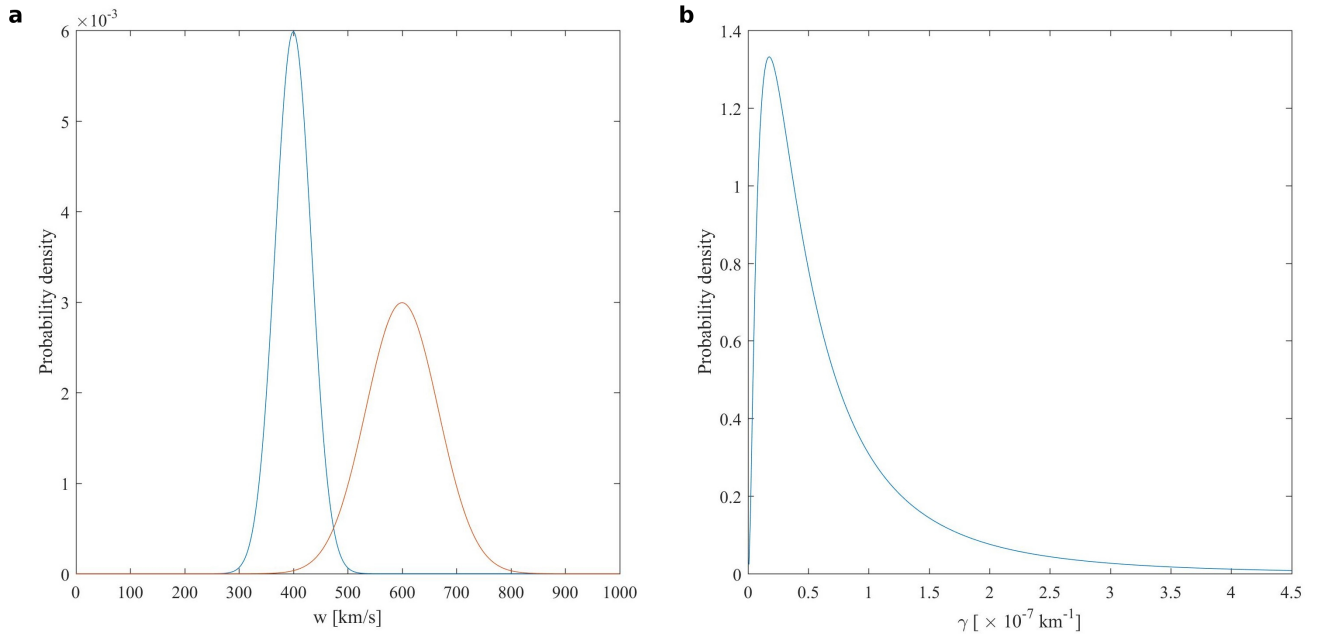

Fig. S1. Left: PDF adopted for the random generation of w in the PDBM, with the slow ω represented by a Gaussian PDF centered at 400km/s with $\sigma = 33$ km/s, and the fast ω represented by a Gaussian PDF centered at 600km/s with $\sigma = 66$ km/s. Right: PDF adopted for the random generation of γ in the PDBM, modeled by a Log-Normal function with $\mu = -0.70$ and $\sigma = 1.01$.

error for ICME time and velocity at arrival (see Fig. 1 as examples of output PDFS).

B. The Validation. To perform a validation of the PDBM, we employed the sample of CMEs from Shi et al. (6). That work provides the travel times from the Sun to Earth, allow the estimation of the initial position and velocity and the associated errors for 21 CMES. In some cases, the travel time had to be corrected, since the authors gave the arrival time of the shock preceding the arrival of the ICME itself by a few hours. These values have been used to generate the r_0 and v_0 PDFs. For each CME the same Log-Normal PDF has been used as in Napoletano et al. (7), while the w PDF has been chosen considering the slow or fast solar wind condition measured at 1AU in the hours before the ICME arrival at Earth. From this data we were able to compute the forecast travel times, the velocity at 1AU and their associated statistical ($\pm 1\sigma$) errors, of the ICMEs in the sample. In Fig. 1 we plot the comparison between the forecast travel times and the measured travel times. Following Shi et al. (6), we highlighted

(in red in the plot) from the whole sample those CME who were likely to have undergone interactions with non-radial forces (e.g.: a possible CME-CME interactions) and were therefore not suitable to be described by the PDBM. In the plot, we also highlighted the perfect match zone, where the forecast and measured travel times are the same within the measure errors. For 10 out of 15 CME of the restricted sample, the absolute differences between measure and forecast travel time is smaller that the forecast error, and the average value of this quantity for the sample is 8.5h.
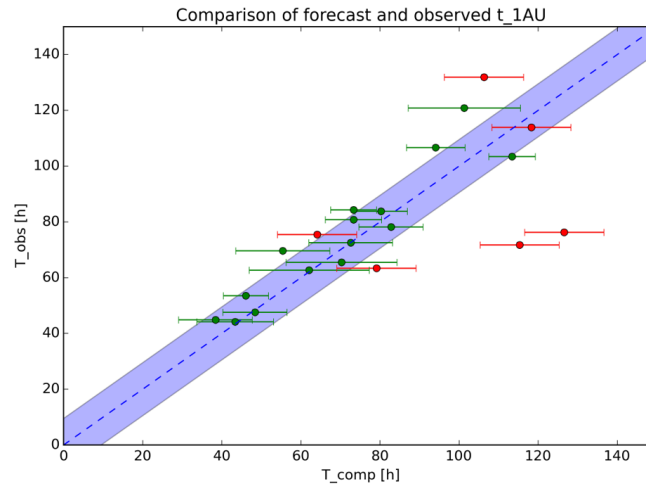

Fig. S2. Dots with error bars are the observed transit times versus forecast transit times from the Shi et al. (6) dataset: in green the restricted sample and in red the CMEs originally excluded from that sample. The dashed line shows the perfect match expectation, with the 1σ travel time measure error zone shaded in blue.

Supplementary Note 3: PDBM real-time implementation

To highlight the capabilities of the PDBM for realtime application, we presented one case study (8), where we compared the forecast provided by the PDBM fed by SOHO/LASCO data and a simple deprojection program with the measured ICME characteristics at its arrival at Earth. Results and graphs from this case study are shown in Figg. S3 and S4. We stress that in the realtime implementation, only information from SDO and SOHO is used to estimate the CME characteristics. This leads to larger errors in the characteristics estimation than when using also information from STEREO, but it is a nice test of the operational capabilities of the PDBM as forecast tool when STEREO data would not be available any more.

Real-time PDBM implementations at present time. PDBM is running in real-time in both IPS (https://ips.telespazio.com/ 9, 10) and SWERTO (http://spaceweather.roma2.infn.it/ 11) Space Weather services. Under SWERTO, the ALICE (ALert for Interplanetary Coronal mass Ejections - at present in beta testing) tool provides an email alert for the arrival of an ICME to various targets in the Heliosphere, upon subscription.
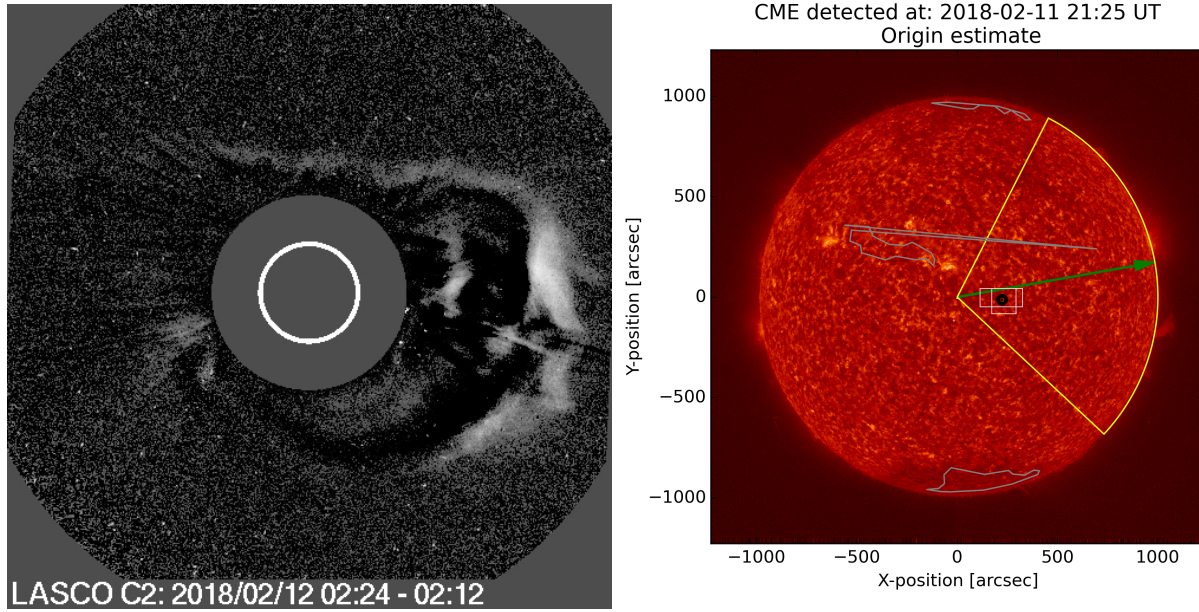
Fig. S3. Left: The 2018 February 12th CME as imaged by the LASCO C2 coronagraph on-board SOHO. The image shown is a contrast enhanced difference of two images acquired few minutes apart. This allows the visualization of the CME front few hours after the onset time. Right: Graphical output of the CME source finding algorithm. We visualize several characteristics of the CME over a SDO/AIA 0304 image of the Sun: the green arrow shows the CME POS angle, the yellow sector shows the angle subtended by the CME POS width, the white boxes and the red dots shows the ARs and recent flare locations, respectively, taken into account to estimate the CME onset location (shown as a black circle). The gray polygons show the position of coronal holes at the time of the CME onset.
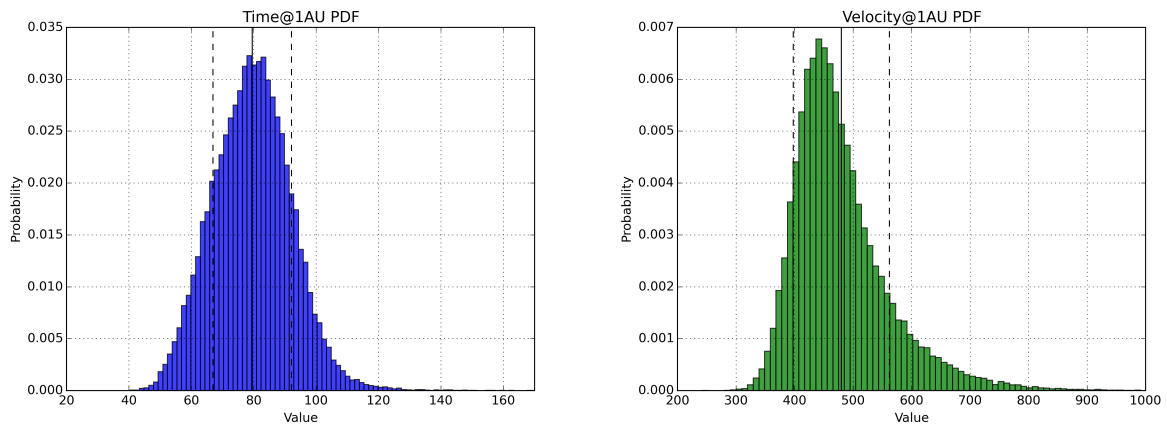

Fig. S4. Left: Probability Density Function of t1AU computed from N=50000 realizations by the PDBM model for the 2018 February 12th CME. The vertical lines indicate the average travel time ($\approx$80h) and the average$\pm$rms values ($\approx$12h). Right: Probability Density Function of v1AU computed from N=50000 realizations by the PDBM model for the 2018 February 12th CME. The vertical lines indicate the average velocity ($\approx$ 480km/s) and the average$\pm$rms values ($\approx$80km/s).

Bibliography

1. Nat Gopalswamy, A Lara, RP Lepping, ML Kaiser, D Berdichevsky, and OC St. Cyr. Interplanetary acceleration of coronal mass ejections. *Geophysical research letters*, 27(2):145–148, 2000.

2. PK Manoharan. Evolution of coronal mass ejections in the inner heliosphere: A study using white-light and scintillation images. *Solar physics*, 235(1-2):345–368, 2006.

3. Peter J Cargill. On the aerodynamic drag force acting on interplanetary coronal mass ejections. *Solar Physics*, 221(1):135–149, 2004.

4. Bojan Vršnak, Tomislav Žic, Dijana Vrbanec, Manuela Temmer, Tanja Rollett, Christian Möstl, Astrid Veronig, Jaša Čalogović, Mateja Dumbović, Slaven Lulić, et al. Propagation of interplanetary coronal mass ejections: The drag-based model. *Solar physics*, 285(1-2):295–315, 2013.

5. Rainer Schwenn, A Dal Lago, Emilia Huttunen, and Walter D Gonzalez. The association of coronal mass ejections with their effects near the earth. 2005.

6. Tong Shi, Yikang Wang, Linfeng Wan, Xin Cheng, Mingde Ding, and Jie Zhang. Predicting the arrival time of coronal mass ejections with the graduated cylindrical shell and drag force model. *The Astrophysical Journal*, 806(2):271, 2015.

7. Gianluca Napoletano, Roberta Forte, Dario Del Moro, Ermanno Pietropaolo, Luca Giovannelli, and Francesco Berrilli. A probabilistic approach to the drag-based model. *Journal of Space Weather and Space Climate*, 8:A11, 2018.

8. Dario Del Moro, Gianluca Napoletano, Roberta Forte, Luca Giovannelli, Ermanno Pietropaolo, and Francesco Berrilli. Forecasting the 2018 february 12th cme propagation with the p-dbm model: A fast warning procedure. *Annals of Geophysics*, 62(4):456, 2019.

9. Carlo Albanese, Filippo Rodriguez, Roberto Ronchini, Stefano di Rollo, Francesco Berrilli, Alice Cristaldi, Dario Del Moro, Roberta Forte, Giorgiana de Franceschi, Claudio Cesaroni, et al. The ionosphere prediction service. In *Space Weather of the Heliosphere: Processes and Forecasts*, volume 335, pages 352–354, 2018.

10. Sreeja Vadakke Veettil, Claudio Cesaroni, Marcio Aquino, Giorgiana De Franceschi, Francesco Berrili, Filippo Rodriguez, Luca Spogli, Dario Del Moro, Alice Cristaldi, Vincenzo Romano, et al. The ionosphere prediction service prototype for gnss users. *Journal of Space Weather and Space Climate*, 9:A41, 2019.

11. Francesco Berrilli, Marco Casolino, Dario Del Moro, Roberta Forte, Luca Giovannelli, Matteo Martucci, Matteo Mergé, Gianluca Napoletano, Livio Narici, Ermanno Pietropalo, et al. Swerto: a regional space weather service. *Proceedings of the International Astronomical Union*, 13(S335):348–351, 2017.